Pharm Res (2015) 32:955–967
DOI 10.1007/s11095-014-1509-x

RESEARCH PAPER

Metal Based Imaging Probes of DO3A-Act-Met for LAT1 Mediated Methionine Specific Tumors : Synthesis and Preclinical Evaluation

K Ganesh Kadiyala • Anupama Datta • Jyoti Tanwar • Anupriya Adhikari • B. S. Hemanth Kumar • Krishna Chuttani • Meganathan Thirumal • Anil K. Mishra

Received: 17 June 2014 / Accepted: 29 August 2014 / Published online: 10 September 2014

ABSTRACT

Purpose Tumor cells are known to have an elevated requirement for methionine due to increased protein synthesis and transmethylation reactions. A methionine based macrocyclic tumor imaging system, DO3A-Act-Met, has been designed to provide a novel platform for tumor imaging via modalities, PET/MRI using metal ions, ^{68}Ga and ^{157}Gd.

Methods Synthesis of DO3A-Act-Met was confirmed through NMR and mass spectrometric techniques. Cytotoxicity of complexes was evaluated using MTT assay whereas receptor binding and trans-stimulation studies were performed on EAT and U-87 MG cell lines. Tumor targeting was assessed through imaging and biodistribution experiments on U-87 MG xenograft model.

Results DO3A-Act-Met was synthesized and radiolabeled with ^{68}Ga in high radiochemical purity (85–92%). The receptor binding assay on EAT cells predicted high binding affinity with K_d of 0.78 nM. Efflux of ^{35}S-L-methionine trans-stimulated by extracellular DO3A-Act-Met on U-87MG cells suggested an L-system transport. MR studies revealed a longitudinal relaxivity of 4.35 mM^{-1} s^{-1} for Gd-DO3A-Act-Met and a 25% signal enhancement at tumor site. The biodistribution studies in U-87MG xenografts validated tumor specificity.

Conclusion DO3A-Act-Met, a methionine conjugated probe is a promising agent for targeted molecular imaging, exhibiting high specificity towards tumor owing to its essential role in proliferation of cancer cells mediated through LAT1.

KEY WORDS cancer · LAT1 · methionine · MRI · PET

ABBREVIATIONS

DOTA	1,4,7,10-tetraazacyclododecane-N, N′,N″, N‴-tetraacetic acid
Ga	Gallium
Gd	Gadolinium
MBq	Megabecquerel
MRI	Magnetic resonance imaging
PET	Positron emission tomography

INTRODUCTION

Molecular imaging techniques are indispensable tools in medical imaging to visualize *in vivo* events that are key in disease prognosis, early diagnosis and monitoring therapeutic responses (1,2). Imaging tools like PET and MRI have proven to be vital aids in tracking the chain of events in a host of disease-specific targets. Cancer has always been of major social health concern and its detection at an early stage is not only crucial but so far the most challenging task for clinicians. Advancement in the design of drugs and molecules for imaging and therapy is dependent on the successful application of target-specific biomolecules utilizing the concept of receptor binding or other *in vivo* interactions. This has led to overwhelming interest in the metabolic imaging of cancer for the search of new diagnosis and treatment procedures (3,4). An interesting target for metabolic tumor imaging is the increased protein metabolism in cancer cells. It majorly arises due to an overexpression of amino acid transporter genes in malignant transformation resulting in increased amino acid transport occurring through carrier mediated processes (5,6).

Electronic supplementary material The online version of this article (doi:10.1007/s11095-014-1509-x) contains supplementary material, which is available to authorized users.

K. Kadiyala • A. Datta (✉) • J. Tanwar • A. Adhikari • B. S. Kumar • K. Chuttani • A. K. Mishra (✉)
Institute of Nuclear Medicine and Allied Sciences, Defence Research and Development Organization, Brig. S.K. Mazumdar Road Delhi 110054, India
e-mail: anupama@inmas.drdo.in
e-mail: akmishra63@gmail.com

K. Kadiyala • J. Tanwar • M. Thirumal
Department of Chemistry, University of Delhi, Delhi 110007, India

Among the different membrane transporter proteins, the ubiquitously found L-type amino acid transporter 1 and 2 (LAT1 and LAT2) transport large neutral amino acids from the extracellular fluids into the cells (7–11). The primary tissues for LAT1 are brain, placenta and tumors while LAT2 is expressed in the kidney, colon and intestine. Due to the high expression of LAT1 in tumor tissue, they are being suitably utilized to gain access into the malignant cells and as carriers for the delivery of the targeted imaging probe (12). The potentiality of these active transporters is further enhanced due to the broad substrate specificity and relatively high transport capacity. LAT1 preferentially transport large neutral amino acids such as phenylalanine, tyrosine, tryptophan and methionine with high affinity in rats (K_m = ~ 10–20 μM) and humans (K_m = ~15–50 μM) (13–15). In this direction, positron emission tomography (PET) with L-(methyl-^{11}C) methionine as a tracer is a commonly used non-invasive metabolic imaging method that has proved its usefulness in detecting several types of malignant human tumors (16,17). The necessity of methionine can be accentuated by the characteristic inability of a variety of human tumor cells to proliferate when methionine is replaced by its immediate precursor homocysteine whereas normal cells grow in such medium (18–21). This absolute "methionine dependency" has always gained attention of the scientist to use methionine as molecule to diagnose and stage various forms of cancers via newly developed methionine based derivatives (22,23). ^{11}C-methioinine though catering the need in diagnoses and monitoring of treatment response, but unfortunately, the short half-life of ^{11}C and its fast metabolism limits the full utilization in the tracer medical imaging.

It was therefore considered prudent to focus our attention on the development of a new methionine imaging system that can be utilized in an imaging techniques viz. PET and MRI for tumor targeting by conjugating L-methionine with a suitable chelate. Among the variety of cyclic and acyclic chelates, both DOTA (24–26) and DTPA (diethylenetriaminepentaacetic acid) (27–29) are indispensable in the development of imaging agents and radiopharmaceuticals, but more emphasis has been given on DOTA complexes due to their significant higher kinetic inertness than DTPA complexes which are known to dissociate and release metal under physiological conditions. Here, we report the synthesis of new ligand, 2,2′,2″-(10-(2-(1-carboxy-3-(methylthio)propylamino)-2-oxoethyl)-1,4,7,10-tetraazacyclododecane-1,4,7-triyl)triacetic acid, DO3A-Act-Met. The designed molecule has been fortified as a methionine based dual-imaging (PET and MRI) probe for tumors after coordinating with suitable metal ion (M^{3+}) of biomedical interest. The final DO3A-Act-Met was complexed with ^{68}Ga and ^{157}Gd and its specificity was assessed *in vitro* by receptor binding and trans-stimulation studies. The potential of DO3A-Act-Met for tumor targeted site specific localization was evaluated *in vivo* by carrying out imaging and biodistribution studies.

MATERIAL AND METHODS

General Material

1,4,7,10-Tetraazacyclododecane was procured from Strem Chemicals Limited (USA). Column chromatography was carried out using silica MN60 (60–200 μm), thin layer chromatography (TLC) was checked on aluminum plates coated with silica gel 60–120, F_{254} (Merck, Germany). For the equilibrium measurements the chemicals used in the experiments were of highest analytical grade. The metal salts, $GdCl_3.6H_2O$, $GaCl_3.xH_2O$ were purchased from Aldrich (99.9%). The stock solution of hydrochloric acid (~0.03 mol dm^{-3}) was prepared from 35% aqueous solution ("puriss" Fluka, Switzerland). M-CSF, soluble RANK, trypsin, EDTA, bovine serum albumin (BSA), fetal bovine serum (FBS) and heat inactivated (Δ)FBS were purchased from Sigma-Aldrich Co (USA) while Dulbecco's medium and streptomycin were procured from Gibco (Grand island, NY) and In-vitrogen Co. respectively. ^{35}S-L-methionine was procured from RCR (northern region), BRIT, Department of Atomic Energy, India. ^{68}Ga was eluted from a ^{68}Ge/^{68}Ga generator (IGG100, Eckert & Ziegler, Germany) with 0.1 N HCl. Spectroscopic studies were carried out by using Bruker Avance II 400 MHz NMR system (Switzerland) and Agilent 6310 ion trap mass spectrometer (mass accuracy ± 0.2 u; USA). Elemental analysis was performed on Elemental analyser system GmbH Vario EL-III instrument. Radiolabeling and biodistribution studies were performed on γ-scintillation counter (GRS230, ECIL, India & Wallac 1480-Wizard 3, Perkin-Elmer, Boston, MA, USA). PET and CT studies were performed on Discovery STE 16 (GE) system. HPLC analysis was performed on Agilent 1200 LC coupled to UV detector (λ = 214 nm). The C-18 RP Agilent column (5 μm, 4 mm × 125 mm) was used along with an isocratic pump. 20% Ammonium acetate (10 mM) and 80% acetonitrile were used as the mobile phase at a flow rate of 2 mL/min. C-18 Cartridges were purchased from Waters Ltd (USA). Beta scintillation counts were obtained by mixing samples in optiphase scintillation cocktail using Wallac Micro beta Trilux 1450LSC, Perkin Elmer (Massachusetts, USA).

Cell Line

Monolayer cultures of human malignant glioma cells, U-87MG, human embryonic (HEK) and Ehrlich Ascites tumor (EAT) cells (obtained from NIMHANS, Bangalore, India) were grown in Dulbecco's medium and RPMI 1640 supplemented with 10% fetal bovine serum (FBS), 100 IU/mL penicillin, 2 mM *L*-glutamine and 100 μg/mL streptomycin. Cells were routinely subcultured twice a week using 0.05% trypsin in 0.02% EDTA.

Animal Model

In vivo procedures were performed according to the protocol approved by the Institutional Animal Ethics Committee (Regn. No: 8/GO/a/99/CPCSEA). New Zealand rabbits of 2–3 Kg were used for blood kinetics studies. Athymic nude mice (age 7–9 weeks, wt. 20–25 g) were used for imaging and biodistribution studies. Mice and rabbits were housed under conditions of controlled temperature of 22±2°C and normal diet. A U-87MG xenograft model was generated by subcutaneous (s.c.) injection of 1×10^6 U-87MG cells in the fore/ hind limb of athymic nude mice which were used three to four weeks after inoculation when the tumor volume was 100–400 mm^3.

Ligand Synthesis

2-(2-Chloro-acetylamino)-4-(methylsulfanyl)-butyric acid methyl ester (1)

To an aqueous solution of L-methionine methyl ester hydrochloride (2.5 mmol, 0.50 g/mL) dissolved in water (10.0 mL), 2-chloroacetyl chloride (3.0 mmol, 0.33 g) in dichloromethane (10.0 mL) and potassium carbonate (6.25 mmol, 0.86 g) in water (10.0 mL) were added simultaneously drop wise with the help of dropping funnels at 0°C over a period of 30 min. The reaction was kept at 0°C for 2 h followed by overnight stirring at RT for 16 h. Finally, the aqueous portion was extracted twice with dichloromethane. The collective organic fractions were separated, dried using Na_2SO_4 and evaporated under vacuum to give compound **1** as a solid in 95.2% yield.

Elemental analysis: Calculated for $C_8H_{14}ClNO_3S$: C, 40.08; H, 5.89; N, 5.84; S, 13.38; found C, 40.12; H, 5.82; N, 5.79; S, 13.42. ^{1}H NMR(400 MHz; $CDCl_3$) 2.0 (1H, m,$-CH_2-$), 2.10 (3H, s, $-S-CH_3$), 2.20 (1H, m, $-CH_2-$), 2.50 (2H, t, $-SCH_2-$), 3.78 (3H, s, $-CH_3$), 4.06 (2H, s, $-COCH_2Cl$), 4.72 (1H, m, $-NCH-$), 7.25 (1H, $-NH-CO-$); ^{13}C NMR(100 MHz; $CDCl_3$)15.47 ($-S-CH_3$), 29.67 ($-CH_2-$), 31.32 ($-CH_2-$), 42.41 ($-CH_3$), 51.83 ($-CH_2Cl$), 52.71 ($-NHCH-$), 165.90 ($-CONH-$), 171.69 ($-COO-$); MS(ESI^+, accuracy: ± 0.2 u): Mass calculated for $C_8H_{14}ClNO_3SNa$ 262.0 $[M+Na]^+$; found 262.2.

1,4,7-Tri(tert-butoxymethane)-1,4,7,10-tetraazacyclododecane (2)

The synthesis was carried out according to the procedure reported in literature (30).

tert-Butyl-2,2′,2″-(10-(2-(1-methoxy-4-(methylthio)-1-oxobutan-2-ylamino)-2-oxoethyl)-1,4,7,10-tetraazacyclododecane-1,4,7-triyl)triacetate (3)

Anhydrous potassium carbonate (2.91 mmol, 0.40 g) was added to a solution of compound **2** in acetonitrile (20 mL) under N_2 atmosphere and heated at 50°C for 30 min. 2-(2-Chloroacetamino)-4-(methylsulfuryl)-butyric acid methyl ester (1.07 mmol, 0.25 g, 1.1 equiv) was slowly added and the reaction was heated to reflux. After 18 h, the reaction was cooled to room temperature, filtered and the filtrate was evaporated under reduced pressure. The crude product obtained was purified by column chromatography (silica gel, 2% methanol in dichloromethane) to give the ligand **3** as a brown solid in 89.5% yield.

Elemental analysis: Calculated for $C_{34}H_{63}N_5O_9S$: C, 56.88; H, 8.84; N, 9.75; S, 4.47; found C, 56.92; H, 8.95; N, 9.71; S, 4.49. ^{1}H NMR(400 MHz; $CDCl_3$) 1.43 (27H, s, $-C(CH_3)_3$), 1.80− 2.45 (14H, m, $-CH_2-$), 2.10 (3H, s, $-S-CH_3$), 2.46–2.75 (7H, broad m,$-CH_2-$), 2.76–3.15 (5H, broad m, $-CH_2-$), 3.16–3.65 (4H, broad m, −CH– and $-CH_2-$), 3.67 (3H, s, $-CH_3$), 4.55 (1H, −NCH−), 8.6 (1H, −NH–CO−); ^{13}**C** NMR(100 MHz; $CDCl_3$)15.37 ($-S-CH_3$), 27.92 ($-CH_3$), 29.66 ($-CH_2-$), 30.59 ($-CH_2-$), 51.76 ($-NCH_2-$), 52.16 ($-CH_2-$), 55.71 (−CH−), 56.05 ($-OCH_3$), 81.85 ($-C(CH_3)_3$), 172.39 (−COO), 172.89 (−CO−); MS(ESI^+): Mass calculated for $C_{34}H_{64}N_5O_9S$ 718.4 $[M+H]^+$; found 718.5.

4-(Methylthio)-2-(2-(4,7,10-tris(2-tert-butoxy-2-oxoethyl)-1,4,7,10-tetraazacyclododecan-1-yl)acetamido)butanoic acid (4)

To a stirred solution of **3** (9.62 mmol, 0.69 g) in methanol (10.0 mL), NaOH solution (2 M) was added slowly till the pH of the reaction mixture reached 12 and the reaction was stirred at room temperature for 12 h. The reaction mixture was then neutralized to pH 7 by addition of dil. HCl solution (2 M) and the organic solvent was evaporated under reduced pressure. The residue obtained was dissolved in dichloromethane and extracted with water. The organic fractions were collected and dried using sodium sulphate. The filtrate obtained was concentrated under reduced pressure to give the desired compound **4** in 92.5% yield. Elemental analysis: Calculated for $C_{33}H_{61}N_5O_9S$: C, 56.31; H, 8.73; N, 9.95; S, 4.56; found C, 56.40; H, 8.69; N, 9.98; S, 4.58. ^{1}H NMR (400 MHz; $CDCl_3$) 1.43 (27H, s, $-C(CH_3)_3$), 1.82–2.45 (14H, broad m,$-CH_2-$), 2.10 (3H, s, $-S-CH_3$), 2.46–3.14 (12H, broad m, $-CH_2-$), 3.18–3.56 (4H, broad m, −CH– and–CH_2-), 4.59 (1H, −NCH−), 9.35 (1H, −NH–CO−); ^{13}C NMR(100 MHz; $CDCl_3$) 15.27 ($-S-CH_3$), 27.91 ($-CH_3$), 29.66 ($-CH_2-$), 48.35 ($-CH_2-$), 52.52 ($-NCH_2-$), 53.45

($-CH_2-$), 55.61 ($-CH-$), 82.11 ($-C(CH_3)_3$), 169.79, 172.47 ($-CO-$), 172.87 ($-COOH$), MS(ESI^+): Mass calculated for $C_{33}H_{62}N_5O_9S$ 704.4 $[M+H]^+$; found 704.5.

2,2′,2″-(10-(2-(1-Carboxy-3-(methylthio)propylamino) -2-oxoethyl)-1,4,7,10-tetraazacyclododecane-1,4,7-triyl) triacetic acid, DO3A-Act-Met

Trifluoroacetic acid (3.0 mL) was taken in a round bottom flask and maintained at 0°C. Compound **4** (0.71 mmol, 0.50 g) was added to the reaction flask and stirred for 4 h at 0°C. The reaction mixture was brought to room temperature and stirred for additional 10 h. Trifluoroacetic acid was evaporated under reduced pressure in presence of methanol (5 mL). The residue obtained was washed three times with dichloromethane to remove any unreacted starting compound. Diethyl ether (30.0 mL) was added drop wise at 0–5°C and stirred for 1 h at room temperature. The compound was dried, dissolved in water and neutralized to pH 7 by the addition of NaOH (1 M). The crude product was finally purified by preparative HPLC to give **DO3A-Act-Met** in 85.3% yield.

Elemental analysis: Calculated. for $C_{21}H_{37}N_5O_9S$: C, 47.09; H, 6.96; N, 13.08; S, 5.99; found C, 47.13; H, 6.89; N, 13.05; S, 6.02. ^{1}H NMR (400 MHz; D_2O): 1.99–2.28 ($-CH_2-$), 2.60 (3H, s, $-S-CH_3$), 2.70–4.40 (22H, br s, $-CH_2-$).^{13}C NMR (100 MHz; D_2O) 23.71 ($-S-CH_3$), 36.30 ($-CH_2-$), 48.41, 48.65, 51.55, 51.66, 53.17, 54.42 ($-CH_2-$), 162.72 ($-CO-$), 163.08 ($-CO-$). MS(ESI^+): Mass calculated for $C_{21}H_{38}N_5O_9SK$ 575.2 $[M+K+H]^+$; found 575.4.

Gd-DO3A-Act-Met

To a stirred aqueous solution of the ligand **DO3A-Act-Met** (0.1 mmol), 1 M NaOH solution was added dropwise until pH 6.5 was attained. A solution of $GdCl_3$ in water was added dropwise in 1: 1 molar ratio. The reaction mixture was heated at 50–60°C for 12 h and the pH of the solution was periodically adjusted to maintain it at 6.5. After 12 h, the reaction mixture was cooled down and then passed through chelex-100 at room temperature. The absence of any free Gd(III) ion was verified by using xylenol orange indicator. The collected fraction of Gd(III) complex was lyophilized to get white solid. MS(ESI^+): Mass calculated for Gd-DO3A-Act-Met 689.1 $[M-H]^+$; found 689.2.

Ga-DO3A-Act-Met

$GaCl_3$ and DO3A-Act-Met were dissolved in water in a stoichiometric ratio of 1:1 and a pH of 4.5 was maintained with acetate buffer (0.01 M). The solution was heated at 90°C for 1 h. The complex thus formed was purified by using a C-18 cartridge and the formed Ga-DO3A-Act-Met was characterized by mass spectrometry. MS(ESI^+): Mass calculated for $^{69/71}$Ga-DO3A-Act-Met 602.1 $[M]^+$; found 602.3.

^{68}Ga-DO3A-Act-Met. Fresh $^{68}Ga^{3+}$ ($t_{1/2}$ 68 min) was eluted from $^{68}Ge/^{68}Ga$ generator system using 0.1 M HCl (740 MBq) and was trapped on a cation exchange Strata X-C cartridge column. The column was washed with 1 mL solution of 80% acetone/0.15 N HCl. $^{68}GaCl_3$ was eluted from the column with a 400 μL mixture of 98% acetone/0.05 N HCl mixture. pH of purified ^{68}Ga(III) complex was adjusted to 4.5 using acetate buffer and stoichiometric amount 100 μg of DO3A-Act-Met was added to the labeling vial. The mixture was heated at 90°C for 10 min. It was cooled and passed through C-18 cartridge (preconditioned with C_2H_5OH and H_2O) to remove excess of free $^{68}GaCl_3$ by washing the cartridge with water (1.0 mL) and finally the Ga-complex was eluted from the cartridge with 200 μL of H_2O/C_2H_5OH (7: 3). The labeling efficiency was checked by ITLC-SG using standard protocol i.e. in CH_3OH/NaOAc (1: 1) and ACN/H_2O (1: 1) solvent system.

Determination of Partition Coefficient

To determine the lipophilicity of the compound radiolabeled DO3A-Act-Met was diluted in 3 mL PBS. An equal volume of 1-octanol was added to obtain a binary system. The system was vortexed for 10 s., mixed gently for another 4 min and then kept aside undisturbed for 15 min for the two layers to separate out. 250 μL ($n=3$) of the sample was taken from each of the layers to determine the radioactivity in a γ-counter. The log P value was calculated with the following formula:

$$\text{Log } P_{\text{octanol/water}} = \log \left(\text{cpm}_{\text{octanol}}/\text{cpm}_{\text{water}}\right).$$

In vitro Stability Experiments

In Phosphate Buffer Solution

Stability of the ^{68}Ga labeled complex was ascertained by taking 100 μL of the labeled compound and mixing it with 2.0 mL of phosphate buffer solution (pH 7.2) followed by incubation at room temperature. The change in radiochemical purity was monitored at different time intervals by ITLC.

In Human Serum

The stability of the labeled compound in human serum was determined by taking blood samples collected from healthy volunteers. The blood was clotted for 1 h at 37°C in a humidified incubator maintaining constant conditions of 5% carbon dioxide and 95% air. The collected samples were

centrifuged at 400*g* for 5 min, and the serum was filtered through 0.22 μm syringe filter into a sterile plastic culture tube. ^{68}Ga-DO3A-Act-Met was mixed with freshly collected human serum, incubated in CO_2 chamber at 37°C and analyzed to check for any dissociation of the complex. The percentage of free ^{68}Ga was estimated using ITLC (acetonitrile and water mixture as mobile phase) and the percentage of dissociation of the complex at different time points in serum was determined.

Cytotoxicity Studies

The cytotoxicity of the DO3A-Act-Met was evaluated by 3-(4,5-dimethylthiazole-2-yl)-2,5-diphenyltetrazolium bromide, MTT colorimetric assay in human embryonic kidney and glioma, U-87MG cells. Exponentially growing cells were plated in a 96-well microtiter plate at a uniform cell density of 4,000 cells/well, 24 h before treatment. Solutions of the compound with different concentrations (varying from nM-mM range) were prepared. Cells were incubated with these solutions for 2 h and MTT assay was performed. At the end of treatment, control and treated cells were incubated with MTT at a final concentration of 0.05 mg/mL for 2 h at 37°C in CO_2 incubator and the medium was removed. The cells were rinsed with PBS buffer, lysed and the formazan crystals formed were dissolved using 150 μL of DMSO. Optical density is measured on 150 μL of extracts at 570 nm (reference filter: 690 nm). The untreated cells were taken as control with 100% viability and cells without addition of MTT were used as blank to calibrate the spectrophotometer to zero absorbance. The relative cell viability (%) compared to control cells was calculated by $A_{sample}/A_{control} \times 100$. Experiment was performed in triplicate and results have been expressed as mean ± SD.

Macrocolony Assay

Monolayer culture of U-87MG cell line was trypsinized and 100 to 1,000 cells were plated depending upon the concentrations of the drug in 60 mm petri-dishes and incubated at 37°C in 5% CO_2 humidified atmosphere for 8 days. Colonies were fixed in methanol and stained with 1% crystal violet. Colonies containing more than 50 cells were counted.

Receptor Binding Studies

Radiolabeled DO3A-Act-Met was checked for its receptor binding specificity towards the EAT carcinoma cell line. The cultured EAT cells (5×10^5 cells/PD) were plated at a uniform cell density and incubated overnight. A monolayer cell line culture was washed thrice with ice cold binding buffer (25 mM HEPES, 10 mM $MgCl_2$ and 1% BSA) at 37°C prior to the experiment. The washed cell line culture was then incubated for 1 h with increasing concentrations of ^{68}Ga-DO3A-Act-Met (0.01–10 μM) in the absence and presence of the 100-fold of excess unlabeled DO3A-Act-Met to get an estimation of total binding and non-specific binding. The difference between the total binding and non-specific binding gave the specific binding. After each experiment, cells were washed with ice-cold binding buffer thrice. Finally, the cells were lysed with 200 μL of lysis buffer and the cell-associated radioactivity counts were determined by gamma scintillation counter. The concentration of the ligand bound to receptors [B] and the free ligand [F] were calculated through the radioactivity counts. Scatchard plot analysis was carried out between the [B]/[F] and [B] based on the following Scatchard equation:

$$\frac{[B]}{[F]} = \frac{-1}{K_d} \times [B] + \frac{R_{total}}{K_d}$$

where, R_{total} is total number of receptors, $-1/K_d$ is the slope.

Trans-stimulation of ^{35}S-L-Methionine

The U-87MG cells were treated with 10 μM (0.37 MBq) ^{35}S-L-methionine for 2 h at 25°C. The already attached methionine was allowed to efflux in HBSS solution in the presence and absence of 0.1 mM DO3A-Act-Met. After completion of the experiment, the cells were washed with ice cold buffer. The cells were digested and amount of methionine left was measured. The intracellular concentration of methionine at time zero was calculated from the sum of effluxed and remaining ^{35}S-L-methionine in cell monolayers.

In vivo Studies

Blood Kinetics

The blood clearance studies were carried out in normal, healthy New Zealand rabbit. 30 MBq of DO3A-Act-Met labeled with ^{68}Ga was administered intravenously through the dorsal ear vein of the animal. Blood was withdrawn through the vein of the other ear at different time intervals starting from 15 min to 6 h and persistence of activity in terms of percentage-administered dose in samples was calculated using gamma well counter.

Scintigraphy Studies

The *in vivo* scintigraphy imaging was performed on U-87MG tumor bearing mice. 3.7 MBq activity was injected in the form of ^{68}Ga-DO3A-Act-Met intravenously through the tail vein of the animal. Imaging of the mice was carried out at different time intervals starting from 30 min.

Biodistribution Studies

The *in vivo* efficacy of DO3A-Act-Met for targeting solid tumor was further checked by biodistribution studies. U-87MG xenografted mice were used for the studies. An aliquot of 9.0 MBq of radiolabeled ^{68}Ga-DO3A-Act-Met was injected in each mice intravenously through the tail vein. The animals were sacrificed by cardiac puncture at different intervals starting from 30 min post injection. Blood samples were collected with the help of a syringe and radioactivity counts were measured. The animals were dissected and the various organs (viz. heart, kidney, stomach, tumor, liver, blood, lungs, spleen, and intestine) were removed, made free from adhering tissue, rinsed with chilled saline, blotted to remove excess liquid, weighed and radioactivity was measured in each organ. The data was expressed as percent administered dose per gram of the organ. For control, biodistribution studies were performed with ^{68}Ga-DO3A using the same procedure. A blocking experiment was performed wherein co-injection with ^{68}Ga-DO3A-Act-Met (5.0 MBq) and DO3A-Act-Met (10 mg/kg) was carried out and the animal was sacrificed after 1 h p.i. The experiments were performed in triplicate.

Relaxation Rate Measurements

The measurement of longitudinal relaxation rate (r_1) of the complex Gd-DO3A-Act-Met were carried out at different concentrations. A stock solution of Gd-DO3A-Act-Met (10 mM) was prepared for relaxometric studies. A set of Gd-complex solution of different concentration (0.25–1 mM) were prepared. The solutions were prepared in phosphate buffered saline of physiological pH 7.2. Relaxation rate measurements were performed at 25°C on a 4.7 T MRI system (Bruker, BioSpec, Switzerland).

Longitudinal (T_1) measurements were performed at 27°C with an inversion-recovery pulse sequence (increment of inversion delay: 10 ms with 456 increments) followed by a RARE imaging sequence (RARE Factor: 16; TR/TE_{eff}: 5000/7.7 ms; FOV: 25×25 mm; matrix: 128×128; slice thickness: 1 mm). T_1 values were measured from six data points generated by inversion recovery pulse sequence. Fitting of T_1 value was done voxel wise on selected ROIs using IGORpro (Wavemetric). The inverse of the relaxation time, ($1/T_1$, s^{-1}) was plotted against Gd(III) concentration (mM) and fitted to a straight line with $R^2>0.99$. The slope of the fitted line was recorded as the relaxivity, r_1.

In vivo MR Imaging

For *in vivo* MR imaging, the animals were divided into two groups for treatment with Gd-DO3A-Act-Met and Gd-DO3A. In the first group, T_1 weighted-spin-echo MR images were acquired before and after intravenous injection of 0.2 mMGd/kg of the contrast agent. The signal enhancement in the various organs was measured over different time periods. During imaging, mice were maintained under anesthesia (1–3% isoflurane) but were allowed to wake up and recover between imaging time points. The tubing containing hot water was positioned under the mouse to keep a constant body temperature. Studies were performed on 7 T MRI system (Bruker, BioSpec 70/30, Switzerland). Standard T_1-weighted multislice multiecho (MSME) scans with Tr=7,000–1,008 ms, TE=9.0 ms, FOV=6×6 mm, matrix=256×256 mm, slice thickness=0.5 mm and interslice distance=0.5 mm. Images were acquired and analyzed using ParaVision 5.1. Regions of interest (ROIs) were drawn over the tumor, normal tissue, and major organs on whole-body coronal images. The mean signal intensity (SI) values was calculated on a region of interest (ROI) manually drawn on the tissue of interest and averaged over three adjacent slices. The mean SI enhancement (Percentage of signal enhancement, SE%) was calculated according to the following equation:

$$SE\% = \frac{Ipost - Ipre}{Ipre} \times 100$$

Where *Ipre* and *Ipost* are the MR signal intensity before and after the injection of the CA. The SE is expressed as percentage normalized by the SE measured at t=0, representing the time at which the first post contrast image has been taken. Contrast-to-noise ratios (CNRs) were calculated using the equation, $CNR=(SI_{tissue}-SI_{muscle})/\sigma_{noise}$, where SI_{tissue} is the signal intensity in the tissue of interest, SI_{muscle} is the signal intensity in the muscle and σ_{noise} is the standard deviation of the noise. CNRs were analysed in two or three axial slices per mouse.

Statistical Analyses

The results are depicted as mean±standard error of the mean (SEM). Statistical analysis was performed using a Student's *t* test. $P<0.05$ was considered significant.

RESULTS

Synthesis of DO3A-Act-Met

The synthetic procedure of DO3A-Act-Met is described in Scheme 1. To achieve our aim of developing a tumor targeted multi-imaging probe, the bifunctional chelate approach was utilized by conjugating a 1,4,7,10-tetraazacyclododecane based derivative with L-methionine. 2-Chloroacetyl chloride was chosen as the source of linkage for this conjugation and was reacted with L-methionine methyl ester to give the α-chloramidederivative of methionine, **I** in 95.2% yield. The

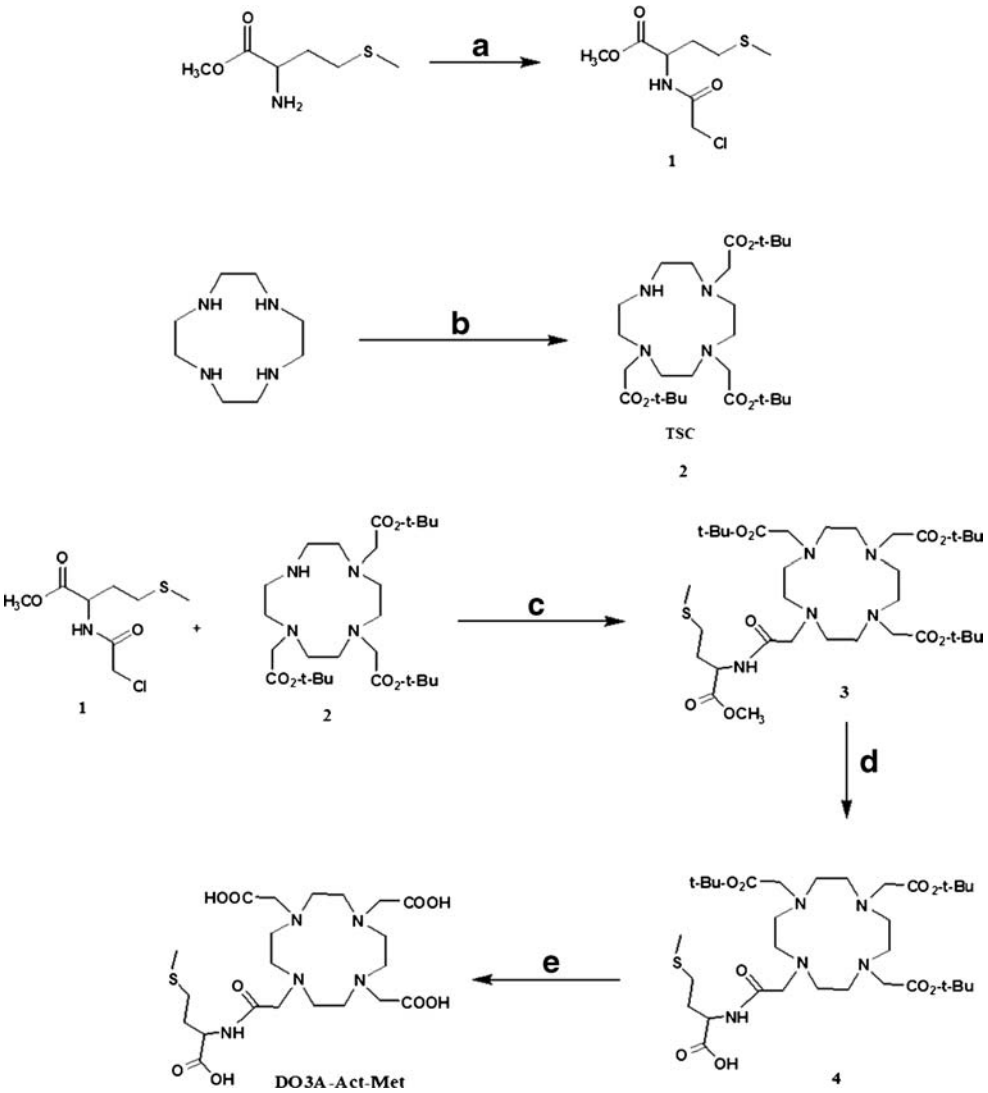

Scheme 1 Synthetic strategy of DO3A-Act-Met. ***Reagents and Conditions***: (**a**) 2-Chloroacetyl chloride, K_2CO_3, DCM/H_2O, 0 °C; (**b**) tert-butylbromoacetate, $NaHCO_3$, acetonitrile, 0°C, 48 h; (**c**) K_2CO_3, acetonitrile, reflux, 18 h; (**d**) 2 M NaOH, methanol, R.T, 12 h; (**e**) TFA, RT, 10 h.

bifunctional chelating agent, 1,4,7-tris(carbobutoxymethyl)-1,4,7,10-tetraaza-cyclododecane, was synthesized by the previously reported reaction of *tert*-butylbromoacetate on 1,4,7,10-tetraaza-cyclododecane (30,31). Its alkylation with the α-chloramide derivative of methionine resulted in compound **3** in 89.5% yield. Further, its methyl ester was hydrolysed in order to obtain the amino acid in its native state, resulting in compound **4** in 92.5% yield. Synthesis of 2,2′,2″-(10-(2-(1-carboxy-3-(methylthio)propylamino)-2-oxoethyl)-1,4,7,10-tetraazacyclododecane-1,4,7-triyl)triacetic acid, DO3A-Act-Met was accomplished in 85.3% yield by the cleavage of *t*-butyl ester groups of 4-(methylthio)-2-(2-(4,7,10-tris(2-*tert*-butoxy-2-oxoethyl)-1,4,7,10-tetraazacyclododecan-1-yl)acetamido)butanoic acid with trifluoroacetic acid (Supplementary Figure S1–S12).

Metal Complexation

For MRI studies, a gadolinium complex of DO3A-Act-Met, was prepared with $GdCl_3 .6H_2O$ in the stoichiometric ratio of 1:1. Elution of the reaction mixture through activated chelex-100 helped to trap free lanthanide ion and provide the neat lanthanide complex of DO3A-Act-Met as the eluent (32,33). The formation of an orange coloured complex confirmed the absence of any free Ln(III) in the Gd complex. For complexation of gallium, stable isotope ^{69,71}Ga isotope was used in the form of $GaCl_3$. Finally, the complex was purified with C-18 cartridge and the formation of the metal complexes of DO3A-Act-Met was confirmed by M^+ ion peak in mass spectrometry. The compound was used as a reference for identification of ^{68}Ga-DO3A-Act-Met complex (Supplementary Figure S13, S14).

Radiochemistry

Labeling with ^{68}Ga

After the formation of $^{69/71}$Ga-DO3A-Act-Met complex was authenticated, DO3A-Act-Met was labeled with ^{68}Ga for

exploring the probe as a PET imaging agent. The labeling efficiency with ^{68}Ga was found to be 87.5% as checked by ITLC and absence of free ^{68}Ga was ensured. The radiochemical purity of ^{68}Ga labeled complex was >96.5% and remained stable for 2 h, after which a decrease of 6% was found in radioactivity over a period of 4 h. The specific activity of ^{68}Ga-DO3A-Act-Met was found to be 3.84 MBq/nmol. The *in vitro* stability in PBS buffer (pH 7.2) and human serum at 37°C was 89.4% and 86.8% respectively after 4 h of incubation. Partition coefficient, log P (pH 7.4) of complex was determined and found to be -1.97±0.2.

Cytotoxicity Studies

The MTT assay was performed to check the effect of the DO3A-Act-Met on cell viability of both cancer and healthy cells at different concentration range. After 2 h incubation with 10 μM DO3A-Act-Met showed a 2.76% and 5.07% loss in viability of HEK and U-87 MG cells whereas at the 1.0 mM level, the exposure resulted in a higher loss in viability of 11.5% and 9.45% respectively. U-87MG and HEK cell lines exhibited survival values of 0.79±0.018 and 0.74±0.015, respectively at 5 mM for unlabeled DO3A-Act-Met in 24 h. The time-dependent curve showed a regain of the metabolic viability of the HEK cell line at 48 h post-treatment at lower concentration of DO3A-Act-Met (Fig. 1).

Receptor Binding Studies

The binding affinity of radiolabeled DO3A-Act-Met was checked on EAT cell line by performing competitive binding assay with unlabeled DO3A-Act-Met. The binding curve showed significant external binding of the labeled DO3A-Act-Met. The affinity of ^{68}Ga-DO3A-Act-Met was revealed by scatchard plot wherein K_d was found to be 0.78 nM (Fig. 2).

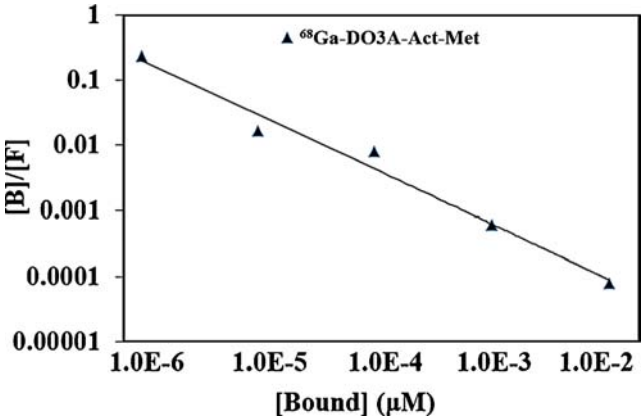

Fig. 2 Receptor binding curve of ^{68}Ga-DO3A-Act-Met on Ehrlich Ascites Tumor cells.

Trans-Stimulation Study of ^{35}S-L-Methionine

To study the efflux activity, experiment was performed on U-87MG cell line using ^{35}S-L-methionine. 10 μM of ^{35}S-L-methionine got incorporated predicting the efflux of ^{35}S-L-methionine was trans-stimulated by extracellular 1 mM of DO3A-Act-Met. The effect was observed to be highest at 60 min and was 0.6026±0.024 μg/mL (Fig. 3).

In vivo Studies

Blood Kinetics Evaluation

In vivo blood clearance of ^{68}Ga-DO3A-Act-Met in rabbits exhibited a somewhat slow trend initially with biological half-life of $t_{1/2}(F)=34.2\pm0.14$ min, but after 4 h the activity had nearly completely washed out from blood, $t_{1/2}(S)=3$ h 25 min±0.19 min (Supplementary Figure S16).

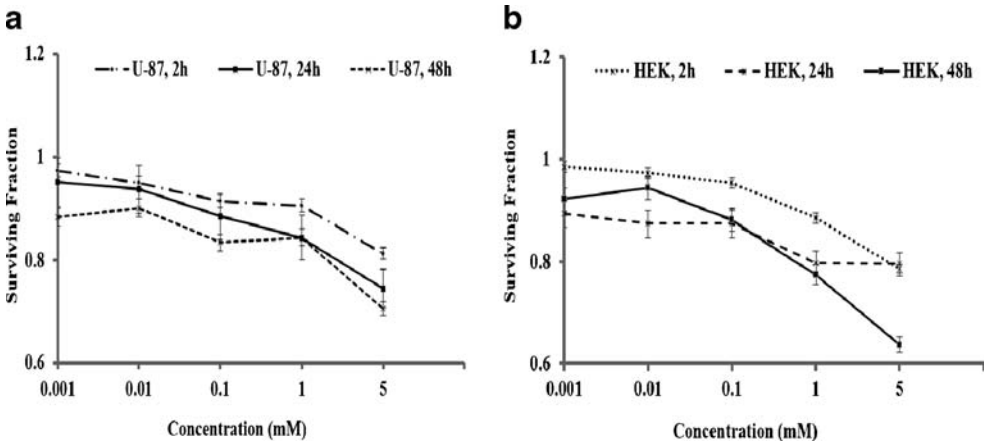

Fig. 1 Cytotoxicity profile of DO3A-Act-Met on (**a**) U-87 MG and (**b**) HEK cells.

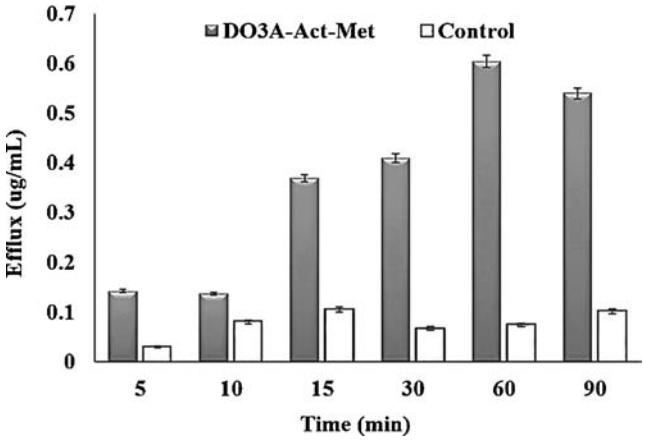

Fig. 3 Trans-stimulation graph of ^{35}S-L-Methionine efflux by extracellular DO3A-Act-Met in U-87MG cells *(□ Control; efflux of ^{35}S-Methionine in absence of DO3A-Act-Met).

In vivo Scintigraphy and Biodistribution Studies

The *in vivo* scintigraphy studies were carried out on U-87MG tumor bearing athymic mice by imaging the animals at different time intervals from 30 min to 3 h p.i. The mice injected with ^{68}Ga-DO3A-Act-Met exhibited uptake in tumor with a gradually increasing trend reaching maximum in 1 h. The accumulation of ^{68}Ga-complex in kidneys and liver was high, with fast washout of the complex. The data correlated well with the data of biodistribution studies. The biodistribution studies in U-87MG tumor bearing athymic mice revealed an initial accumulation of ^{68}Ga complex in kidney was 10.56±1.11% ID/g, (Figs. 4 and 5a) however post 1 h, 6.2±0.82% ID/g of ^{68}Ga-DO3A-Act-Met was left in kidneys. The studies revealed uptake of ^{68}Ga complex in tumor was maximum at 1 h with 2.14±0.25% ID/g uptake. The retention of ^{68}Ga complex in the blood during initial 30 min was high, with 4.79 ±0.27% ID/g at 30 min but came down to 1.64±0.17% ID/g at 1 h p.i. The localization of radioactivity in spleen, stomach and small intestine was low, less than 2% ID/g at 1 h suggesting the specificity of DO3A-Act-Met. As control, the distribution of ^{68}Ga-DO3A into various organs was also studied. The uptake in the kidneys was 8.45±0.3% ID/g and 3.52±0.5% ID/g at 30 min and 1 h respectively. The uptake in liver was less than 1.5% ID/g at all time points. The accumulation in tumor was 0.55±0.3% ID/g at 1 h. The uptake in U-87MG tumor in the presence of non labeled DO3A-Act-Met was found to be 0.9±0.3% ID/g at 1 h and was significantly lower than without blocking 2.14±0.25% ID/g.

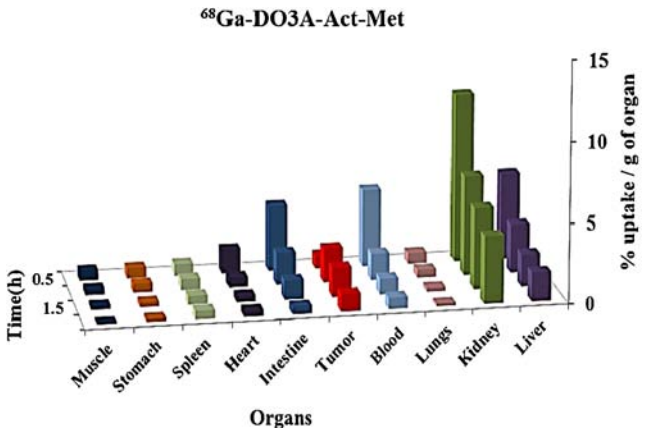

Fig. 4 Biodistribution profile of ^{68}Ga-DO3A-Act-Met in U-87MG xenograft bearing athymic mice.

Relaxation Studies

A stock solution of Gd-DO3A-Act-Met (10 mM) was prepared for relaxometric studies at pH 7.0 using KMOPS buffer. The buffered Gd-DO3A-Act-Met solution was allowed to equilibrate for 30 min and longitudinal (T_1) relaxation time of solvent-water protons was measured as a function of variable Gd-DO3A-Act-Met concentration (0.1–1.0 mM) to investigate its relaxation behaviour. A plot of relaxivity as a function of Gd-DO3A-Act-Met concentration showed linear enhancement in relaxivity with the concentration of the gadolinium complex. The longitudinal relaxivity, r_1 value of Gd-DO3A-Act-Met was found to be 4.35 mM^{-1} s^{-1} (Supplementary Figure S15).

In vivo MR Imaging

To establish whether Gd-DO3A-Act-Met would increase contrast-to-noise ratio (CNR) of tumor *in vivo*, xenografted mice were injected with Gd-DO3A-Act-Met through the tail vein and their images were acquired at different time intervals (Fig. 5b and c). As a control, the second group of tumor bearing mice were injected with the same dose of Gd-DO3A. The variation in the signal enhancement was measured as a function of time (Fig. 6). The analysis of the xenografted images revealed that after injection of the agent all the organs exhibited signal enhancement. As seen from the enhancement the accumulation of the imaging agent started within 30 min. of injection in both the control and DO3A-Act-Met in similar pattern though the intensity was higher in case of DO3A-Act-Met. This enhancement of the signal remained static or unchanged for the next 1 h in both the agents, however post 2 h, Gd-DO3A exhibited a steep decay in signal intensity in the organs and became negligible in 3 h. At 2 h p.i., Gd-DO3A-Act-Met exhibited enhancement of signal in the tumor cells by 25% while the percentage of enhancement was close to 20 in kidneys and muscles. This enhancement of the signal remained static till 3 h in tumor tissues. However, fast decay in signal intensity was noticed in the kidneys and muscle due to the wash out of DO3A-Act-Met and the signal enhancement percentage dropped to 10.4%

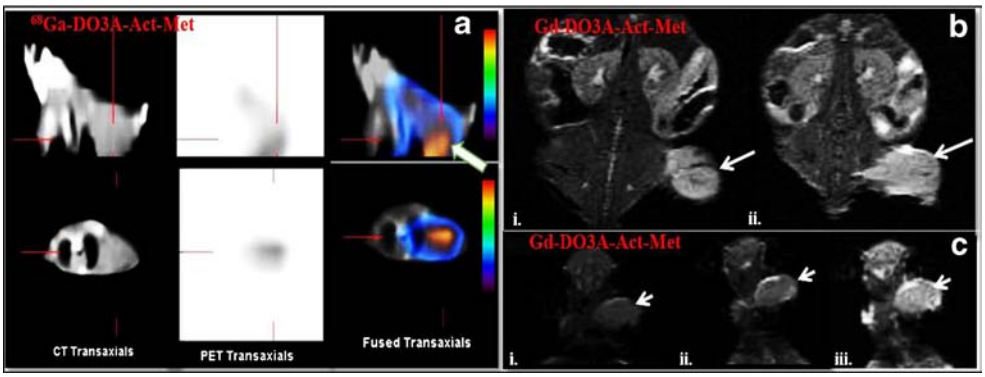

Fig. 5 Representative images of (**a**) PET/ CT (coronal and transaxial) image, 1 h p.i. (**b**) MRI images: *i*. 1 h, *ii*. 2 h p.i. (**c**) Time course MR signal enhancement at the site of tumor: *i*. Control; *ii*. 1 h; *iii*. 2 h p.i. (*Arrow depicts the site of tumor).

and 7% respectively. Markedly, the intensity remained constant in tumor during that period, leading to increase in CNR at the site of tumor at 3 h consequently enhancing the contrast noticeably at the site of tumor. Such behaviour was suggestive of a relatively slower wash out from the tumor than other organs. The percentage signal enhancement in all the organs was <5% at 6 h.

DISCUSSION

Metal based imaging techniques like PET (with ^{68}Ga, ^{11}C, ^{18}F, ^{64}Cu) and MRI (^{157}Gd) are considered sensitive techniques for *in vivo* imaging of ligand-receptor interaction. With the aim to leverage the amino acid transport imaging (LAT1/LAT2) via an increased protein metabolism in cancer cell caused by the chain of events leading to overexpression of variety of transporters and receptors, an amino acid based probe was developed wherein L-methionine was employed owing to its essential role in proliferation of cancer cells. As, DOTA like ligands can be used for complexation of a large group of metal ions (lanthanides, as well as many transition or main group metal ions), the properties of the probe can be easily tuned for varied applications by appending target specific groups to its functionalities. Conjugation of 1,4,7,10-tetraazacyclododecane based derivative with L-methionine to develop a multiutility probe for tumor targeting is the main focus of this work. A number of methodologies are known for conjugating biomolecules to 1,4,7,10-tetraazacyclododecane and its derivatives. However in our synthetic approach, 2-chloroacetyl chloride has been utilized as the linkage, due to easy availability of its two reactive claws for alkylation reactions with simple and straight forward procedure (31). Also, it will be a vital linker between methionine and macrocyclic moiety providing the biocompatible amide linkage prevalent widely in the *in vivo* system in the form of the protein linkage (34). The choice of methyl ester of methionine precursor not only gave enhanced solubility in organic solvents whilst minimising the likelihood of possible side reactions. The formation of the compound was ascertained by appearance of the carbonyl peak–CO–NH at 162.7 ppm in ^{13}C spectrum. The mass spectrum at m/z 575.4 further confirms the same.

DO3A-Act-Met has the DO3A framework which can well be utilized to check the tumor targeted properties in different molecular imaging techniques after complexing with appropriate metal ion. DO3A based compounds are known to form well defined complexes with lanthanide metals with +3 oxidation state and their ^{68}Ga and ^{157}Gd based complexes have been well exploited in PET and MR imaging. Also, the fact that the production of ^{18}F and ^{11}C require cyclotron and chemical processing which are difficult and expensive to maintain, we extended the study towards PET imaging by

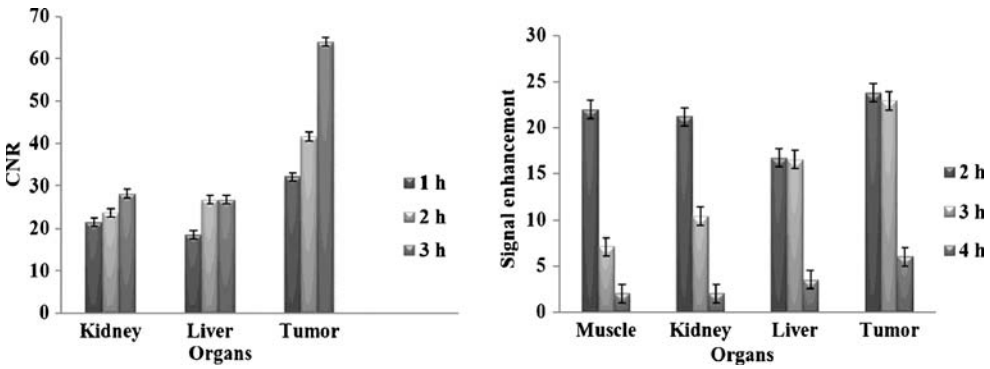

Fig. 6 CNR and Signal enhancement of Gd-DO3A-Act-Met in different organs of U-87 MG xenografted athymic mice at different time intervals.

radiolabeling the probe with ^{68}Ga wherein ^{68}Ga can be produced using a cost effective option of generator system which is relatively easily available. Therefore, DO3A-Act-Met was complexed with ^{68}Ga and ^{157}Gd for the evaluation of tumor seeking properties. The ^{68}Ga-DO3A-Act-Met showed high radiochemical purity of more than 90% and a reasonably good *in vitro* stability of ≥90%. The stability was sufficiently high for *in vitro* and *in vivo* experiments as the complexes exhibited negligible detachment in PBS buffer and human serum.

Since the title compound was designed for tumor imaging, to assess whether DO3A-Act-Met is effectively taken up by tumor cells, *in vitro* cellular internalization studies were performed. It has been proposed that amino acid transporters are upregulated to support high-level protein synthesis for continuous growth and proliferation. The L-type amino acid transport system was originally identified in Ehrlich Ascites carcinoma cells, thus they were selected for preliminary studies (35,36) and further studies were extrapolated to LAT1 receptors rich human glioma, U-87MG cells (37). The degree of cellular internalization of the complex is an important parameter to predict its uptake in the tumor cells by a receptor/transporter mediated process. Prior to these cellular studies the stability of radioactive complexes were evaluated by incubation in the cell growth medium. Radiometric TLC analysis confirmed that the complex was stable in these conditions during the incubation period. The receptor binding studies of DO3A-Act-Met conjugate to evaluate the effect of the chemical modification on the biological activity of methionine were performed. The binding (K_d) on malignant cancer cell lines was found to be in nanomolar range as suggested by scatchard analysis verifying the strong affinity of the probe. The specificity of the internalization was indeed due to the presence of the methionine group in the designed compound was validated by trans-stimulation studies performed with ^{35}S-L-methionine. The increase in efflux of ^{35}S-L-methionine from the U-87MG cell lines in the presence of suggested that the presence of DO3A-Act-Met in the culture medium significantly trans-stimulated the efflux of ^{35}S-L-methionine. These analyses highlighted the biological activity of the probe and validated our results that its transportation across the cell membrane takes place against a concentration gradient and not just by passive diffusion. *In vivo* blood kinetics study performed on rabbits shows a slow trend for activity washout of ^{68}Ga-DO3A-Act-Met. The U-87MG tumor bearing athymic mice used for scintigraphy and biodistribution studies were a vital aid in screening of biological profile and judge the potential of the complex as tumor imaging agent. The *in vivo* scintigraphy images of the xenografted mice correlated well with their tissue distribution profile. Though the initial accumulation of ^{68}Ga-DO3A-Act-Met in kidney and liver was high but a remarkable wash out of activity was seen from liver after 1 h suggesting that radiotracer was mainly excreted through the renal route. The tumor-to-nontumor (T/NT) ratio of ^{68}Ga-DO3A-Act-Met was significantly high (5.94). In addition, observed activity depletion was rapid in blood, the trend was similar to the blood kinetics in rabbit where ~70% of the activity washed out in 30 min showing a good plasma pharmacokinetics. The comparison of biodistribution data with ^{68}Ga-DO3A suggested the modification leads to a significant change in distribution of tracer in various organs. These data demonstrated that ^{68}Ga-DO3A-Act-Met has accumulated more in blood compared to ^{68}Ga-DO3A, and unlike ^{68}Ga-DO3A is excreted through both the renal and the hepatobiliary routes. The higher accumulation in reticularendothelium system organs such as liver and spleen could be corroborated to the lipophilic nature of the probe and is also the characteristics of methionine based derivatives (29,38). The tumor/muscle ratio was approximately 1.5 and 6 fold greater for ^{68}Ga-DO3A-Act-Met at 30 min and 60 min post-injection respectively, suggest that ^{68}Ga-DO3A-Act-Met accumulates significantly into the tumor when compared to ^{68}Ga-DO3A possibly mediated via the LAT1 transporters.

The blocking experiment with cold DO3A-Act-Met clearly showed the specificity of DO3A-Act-Met as the U-87MG tumor uptake was significantly lower in the presence of non radiolabeled DO3A-Act-Met. The suitability of DO3A-Act-Met as a MRI probe was assessed by complexing it with gadolinium to form, Gd-DO3A-Act-Met. Contrast enhanced MRI allowed non invasive visualization of real time pharmacokinetics and biodistribution of the paramagnetically labeled Gd(III) chelate with high special resolution. The r_1 value is slightly higher than those of $[Gd(DOTA)(H_2O)]^{-1}$ (4.02 mM^{-1} s^{-1} per Gd, 25°C) and $[Gd(DTPA)(H_2O)]^{-1}$ (4.22 mM^{-1} s^{-1} per Gd, 25°C) (39) which could possibly be because of the increased molecular weight and interaction volume. The MRI images of the *in vivo* xenografted mice displayed significant and tissue specific enhancement. The changes in signal intensity of the gadolinium complex after injection of the DO3A-Act-Met were comparable to or greater than the changes seen after injection of DO3A for the initial time point. Unlike DO3A, the *in vivo* retention of the probe was longer and tumor targeted. Also, the wash out kinetics of the probe from muscle and non-target organ was much rapid than from the tumor. *In vivo* signal enhancement in MRI data clearly showed that Gd-DO3A-Act-Met demonstrated enhanced retention in the tumor with time with respect to the untargeted control Gd-DO3A, whereas such behaviour was not seen in muscles. Consequently, the preferential retention led to enhanced CNR over the time due to the decrease in the signal intensity in the non target organs while the intensity remained constant in tumor with time. It confirmed the affinity of the probe towards tumor cells and the longer retention time within the tumor microenvironment is in line with the preferential internalization of Gd-DO3A-Act-Met into the tumor cells.

CONCLUSIONS

For effective utilization of imaging agents from bench to human applications a better understanding of their *in vivo* behaviour is essential. With this background, the current work was designed to target metabolic tumor imaging via an increased protein metabolism in cancer cells. It was demonstrated that L-methionine could be efficiently coupled with DO3A using a facile methodology to give DO3A-Act-Met in high yield. This molecule exploits the essential role of L-methionine in cellular metabolism to produce enhanced tumor targeting. The efficacy of the ligand was proved by its successful radiolabeling with cost effective generator based radioisotopes that ensured minimal cytotoxicity and significant cellular uptake in U-87MG cancer cells. Its preferred stable complexation with metals further expands its suitability for different imaging modalities viz. PET and MRI. Receptor binding studies suggests the participation of LAT1 in tumor uptake. This observation can prove helpful for future biological evaluation on this molecule. To understand tumor pathogenesis, the same imaging probe can be utilized for the comparison of relevant information obtained through different imaging modalities. The DO3A-Act-Met developed as part of this study is effective for contrast enhanced tumor imaging with the same agent and the feasibility of being used on different platforms and time scales could be of paramount importance.

ACKNOWLEDGEMENTS

This work was made possible by a financial contribution from DRDO, project INM-311.3.1 and Council of Scientific and Industrial Research. We thank Dr. R. P. Tripathi, Director, Institute of Nuclear Medicine and Allied Sciences, Defence Research and Development Organization for providing the research facilities.

Conflict of Interest The authors declare no competing financial interest.

REFERENCES

1. Nolting DD, Nickels ML, Guo N, Wellington P. Molecular imaging probe development: a chemistry perspective. Am J Nucl Med Mol Imaging. 2012;2(3):273–306.
2. Morrissey S. Targeting cancer. Chem Eng News Archive. 2004;82(38):13.
3. Zhuang H, Pourdehand M, Lambright ES, Yamamoto AJ, Lanuti M, Li PP, *et al.* Dual time point 18F-FDG imaging for differentiating malignant from inflammatory processes. J Nucl Med. 2001;42(9): 1412–17.
4. Pandit N, Gonen M, Krug L, Larson SM. Prognostic value of [18F]FDG-PET imaging in small cell lung cancer. Eur J Nuc Med Mol Imaging. 2003;30(1):78–84.
5. Busch H, Davis JR, Honig GR. The uptake of a variety of amino acids into nuclear proteins of tumors and other tissues. Cancer Res. 1959;19:1030–39.
6. Milton H, Saier J, Gregory AD, Paula B, Joan L. Neutral amino acid transport systems in animal cells: potential targets of oncogene action and regulators of cellular growth. J Membrane Biol. 1988;104(1):1–20.
7. Kanai Y, Segawa H, Miyamoto K, Uchino H, Takeda E, Endou H. Expression cloning and characterization of a transporter for large neutral amino acid activated by the heavy chain 4F2 antigen (CD98). J Biol Chem. 1998;273(37):23629–32.
8. Eva DAP, Urtti A, Yliperttula M. Pharmacokinetic role of L-type amino acid transporters LAT1 and LAT2. Eur J Pharm Sci. 2008;35(3):161–74.
9. Yoon JH, Kim IJ, Kim H, Kim HJ, Jeong MJ, Ahn SG, *et al.* Amino acid transport system L is differentially expressed in human normal oral keratinocytes and human oral cancer cells. Cancer Lett. 2005;222(2):237–45.
10. Fuchs BC, Bode BP. Amino acid transporters ASCT2 and LAT1 in cancer: partners in crime? Semin Cancer Biol. 2005;15(4):254–66.
11. Kanai Y, Endou H. Heterodimeric amino acid transporters: molecular biology and pathological relevance. Curr Drug Metab. 2001;2(4):339–54.
12. Nawashiro H, Otani N, Shinomiya N, Fukui S, Ooigawa H, Shima K, *et al.* L-type amino acid trasporter 1 as a potential molecular target in human astrocytictumors. Int J Cancer. 2006;119(3):484–92.
13. Yanagida O, Kanai Y, Chairoungdua A, Kim DK, Segawa H, Nii T, *et al.* Human L-type amino acid transporter 1 (LAT1): characterization of function and expression in tumor cell lines. Biochim Biophys Acta. 2001;1514(2):291–302.
14. Uchino H, Kanai Y, Kim DK, Wempe MF, Chairoungdua A, Morimoto E, *et al.* Transport of amino acid-related compounds mediated by L-type amino acid transporter 1 (LAT1): insights into the mechanisms of substrate recognition. Mol Pharmacol. 2002;61(4):729–37.
15. He S, Tang G, Hu K, Wang H, Wang S, Huaang T, *et al.* Radiosynthesis and biological evaluation of 5-(3-[(18)F]Fluoropropyloxy)-L-tryptophan for tumor PET imaging. Nucl Med Biol. 2013;40(6):801–07.
16. Singhal T, Narayanan TK, Jain V, Mukherjee J, Mantil J. 11C-L-Methionine positron emission tomography in the clinical management of cerebral gliomas. Mol Imaging Biol. 2008;10(1):1–18.
17. Kracht LW, Friese M, Herholz K, Schroder R, Bauer B, Jacobs A, *et al.* Methyl-[11C]-L-methionine uptake as measured by positron emission tomography correlates to microvessel density in patients with glioma. Eur J Nucl Med Mol Imaging. 2003;30(6):868–73.
18. Kreis W, Goodenow M. Methionine requirement and replacement by homocysteine in tissue cultures of selected rodent and human malignant and normal cells. Cancer Res. 1978;38:2259–62.
19. Mecham J, Rowitch D, Wallace CD, Stern PH, Hoffman RM. The metabolic defect of methionine dependence occurs frequently in human tumor cell lines. Biochem Biophys Res Commun. 1983;117(2):429–34.
20. Hoffman RM. Altered methionine metabolism and transmethylation in cancer. Anticancer Res. 1985;5(1):1–30.
21. Judde JG, Ellis M, Frost P. Biochemical analysis of the role of transmethylation in the methionine dependence of tumor cells. Cancer Res. 1989;49:4859–65.
22. Leskinen-Kallio S, Nagren K, Lehikoinen P, Ruotsalainen U, Joensuu H. Uptake of 11C-methionine in breast cancer studied by PET. An association with size of S-phase fraction. Br J Cancer. 1991;64(6):1121–24.
23. Leskinen-Kallio S, Nagren K, Lehikoinen P, Ruotsalainen U, Teras M, Joensuu H. Carbon-11-methionine and PET is an effective method to image head and neck cancer. J Nucl Med. 1992;33(5):691–95.

24. Jang YH, Blanco M, Dasgupta S, Keire DA, Shively JE, Goddard WA. Mechanism and energetics for complexation of ^{90}Y with 1,4,7,10-Tetraazacyclododecane-1,4,7,10-tetraacetic acid (DOTA), A model for cancer radioimmunotherapy. J Am Chem Soc. 1999;121(26):6142–51.
25. Perols A, Honarvar H, Strand J, Selvaraju R, Orlova A, Karlström AE, *et al.* Influence of DOTA chelator position on biodistribution and targeting properties of 111In-labeled synthetic anti-HER2 affibody molecules. Bioconjugate Chem. 2012;23(8):1661–70.
26. Adhikari A, Datta A, Adhikari M, Chauhan K, Chuttani K, Saw S, *et al.* Preclinical evaluation of DO3A-Act-AQ: A polyazamacrocyclic monomeric anthraquinone derivative as theranostic agent. Mol Pharm. 2014;11(2):445–56.
27. Boden V, Colin C, Barbet J, Doussal JML, Vijayalakshmi M. Preliminary study of the metal binding site of an anti-dtpa-indium antibody by equilibrium binding immunoassays and immobilized metal ion affinity chromatography. Bioconjugate Chem. 1995;6(4):373–79.
28. Bovens E, Hoefnagel MA, Boers E, Lammers H, Bekkum HV, Peters JA. Multinuclear magnetic resonance study on the structure and dynamics of lanthanide(III) complexes of cyclic DTPA derivatives in aqueous solution. Inorg Chem. 1996;35(26):7679–83.
29. Hazari PP, Shukla G, Goel V, Chuttani K, Kumar N, Sharma R, *et al.* Synthesis of specific SPECT-radiopharmaceutical for tumor imaging based on methionine: ^{99m}Tc-DTPA-bis(methionine). Bioconjugate Chem. 2012;21(2):229–39.
30. Tanwar J, Datta A, Tiwari AK, Thirumal M, Chuttani K, Mishra AK. Preclinical evaluation of DO3P-AME-DO3P: a polyazamacrocyclic methylene phosphonate for diagnosis and therapy of skeletal metastases. Bioconjugate Chem. 2011;22(2):244–55.
31. Leon-Rodriguez LMD, Kovacs Z. The Synthesis and chelation chemistry of DOTA–peptide conjugates. Bioconjugate Chem. 2008;19(2):391–402.
32. Lu ZR, Wang X, Parker DL, Goodrich KC, Buswell HR. Poly(L-glutamic acid) Gd(III)-DOTA conjugate with a degradable spacer for magnetic resonance imaging. Bioconjugate Chem. 2003;14(4):715–19.
33. Sherry AD, Brown RD, Geraldes CFGC, Koenig SH, Kuan KT, Spiller M. Synthesis and characterization of the gadolinium (3+) complex of DOTA-propylamide: a model DOTA-protein conjugate. Inorg Chem. 1989;28(3):620–22.
34. Krakowiak KE, Bradshaw JS. Synthesis of azacrownmacrocycles and related compounds by a crablike cyclization method: a short review. Ind Eng Chem Res. 2000;39(10):3499–507.
35. Oxender DL, Christensen HN. Evidence for two types of mediation of neutral and amino-acid transport in Ehrlich cells. Nature. 1963;197:765–67.
36. Ylikangas H, Peura L, Malmioja K, Leppanen J, Laine K, Poso A, *et al.* Structure-activity relationship study of compounds binding to large amino acid transporter 1 (LAT1) based on pharmacophoremodeling and in situ rat brain perfusion. Eur J Pharm Sci. 2012;48(3):523–31.
37. Lee JJ, Shetty D, Lee YS, Kim SE, Kim YJ, Hong MK, *et al.* Evaluation of (111)In-labeledmacrocyclicchelator-amino acid derivatives for cancer imaging. Nucl Med Biol. 2012;39(3):325–33.
38. Borbas KE, Ferreira CSM, Perkins A, Bruce JI, Missailidis S. Design and synthesis of mono- and multimeric targeted radiopharmaceuticals based on novel cyclen ligands coupled to anti-muc1 aptamers for the diagnostic imaging and targeted radiotherapy of cancer. Bioconjugate Chem. 2007;18(4):1205–12.
39. Tóth E, Helm L, Merbach A. Relaxivity of gadolinium (III) complexes: theory and mechanism. In: Merbach A, Helm L, Tóth E, editors. The chemistry of contrast agents in medical resonance imaging. United Kingdom: John Wiley and Sons Ltd; 2013. p. 35–71.